Electroabsorption Spectra of Quantum Dots of PbS and Analysis by the Integral Method

ARTICLE *in* THE JOURNAL OF PHYSICAL CHEMISTRY C · FEBRUARY 2015

Impact Factor: 4.77 · DOI: 10.1021/jp5116977

3 AUTHORS, INCLUDING:

Kamlesh Awasthi

National Chiao Tung University

19 PUBLICATIONS **47** CITATIONS

SEE PROFILE

THE JOURNAL OF PHYSICAL CHEMISTRY C

Article

pubs.acs.org/JPCC

Electroabsorption Spectra of Quantum Dots of PbS and Analysis by the Integral Method

Kamlesh Awasthi,[†] Toshifumi Iimori,[‡] and Nobuhiro Ohta*[,†]

[†]Research Institute for Electronic Science (RIES), Hokkaido University, Sapporo 001-0020, Japan

[‡]Department of Applied Chemistry, Muroran Institute of Technology, Muroran 050-8585, Japan

Supporting Information

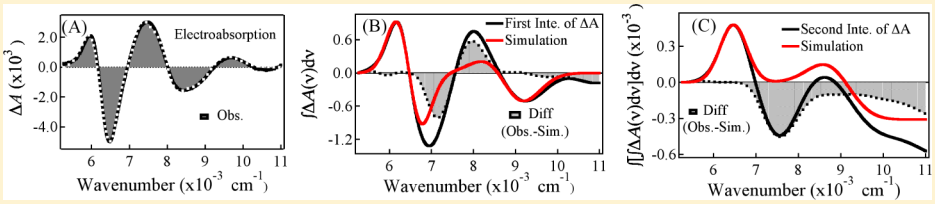

ABSTRACT: Electroabsorption (E-A) spectra of semiconductor quantum dots (QDs) of PbS have been analyzed by the integral method, which is powerful not only to determine the change in electric dipole moment and/or polarizability following absorption precisely but also to confirm the weak absorption bands buried under other strong absorption bands. In the results, two weak absorption bands which induce blue-shift and red-shift, respectively, with application of electric fields have been newly confirmed in PbS QDs to be located just above the intense first exciton band. The energy separation between these two bands becomes smaller, as the applied field strength becomes stronger, suggesting that the interaction between the states excited by these transitions becomes weaker by application of electric fields. The QD size dependence has been reported both for the transition energy and for the magnitude of the change in electric dipole moment and molecular polarizability following the absorption of each band. The assignment of the absorption bands has also been discussed.

INTRODUCTION

Quantum dots (QDs) represent the ultimate in semiconductor-based quantum-confined systems, and great focus has been received during the last two decades because of unique optical and electronic properties as well as their possibilities in various applications such as optoelectronic devices and biological imaging.[1−11] Quantum confinement transforms the band structure of the bulk semiconductor into a series of discrete transitions, which makes it possible to manipulate the energetic positions of the optical transitions of semiconductor QDs by changing the size.

In recent years, much attention has been paid to lead chalcogenide colloidal QDs.[12−19] Their rock-salt lattice leads to an electronic band structure, which is different from those of the typical II−VI compounds, with important consequences for the optical and electrical properties in the regime of strong confinement. Furthermore, lead chalcogenide QDs hold promise for a number of opto-electrical applications in the near-infrared (NIR) region. Lead sulfide (PbS), which is a direct band gap semiconductor material with a rather small bulk band gap (0.41 eV) and a large excitation Bohr radius (20 nm), has attracted much attention due to its wide potential applications in optical devices as optical switches, NIR communication, thermal and biologic images, and photovoltaic solar cells, etc.[18,19]

External electric field effects on optical spectra have been extensively used in molecular spectroscopy to examine electronic structures in the excited states.[20−23] The so-called electroabsorption (E-A) spectra provide unique information about the difference in electric dipole moment (μ) and molecular polarizability (α) between the ground state and the excited state. E-A measurements have been used by many research groups to investigate the electric-field effects on the electronic states in II−VI semiconductor QDs across the visible spectral range (400−800 nm), such as CdS, CdSe, ZnSe, CdS_xSe_{1-x}, etc.[24−34] E-A spectra in the near-infrared region were also reported for PbS and PbSe.[35,36] Narrow transition line widths inherent in QDs, coupled with large Stark shift, should result in electro-optic modulation devices with even greater efficiency. In addition to possible device applications, the quantum-confined Stark effect (QCSE) can be used to prove the nature of the excited states of QDs.

For the determination of the electric dipole moment, molecular polarizability, transition moment polarizability, or transition moment hyperpolarizability from the measured absorption and E-A spectra, a model-based fitting of the simulated spectra to the measured ones is needed. A theory of the electric field effects on the absorption of polarized light by an ensemble of mobile molecules at thermal equilibrium was first developed by Liptay.[22] It was shown that E-A and absorption spectra of a given electronic transition are related to each other so that the E-A spectrum can be expressed as a linear

Received: November 22, 2014
Revised: January 25, 2015
Published: February 10, 2015

DOI: 10.1021/jp5116977
J. Phys. Chem. C 2015, 119, 4351−4361

combination of the zeroth, first, and second derivatives of the absorption spectrum as a function of the excitation light wavenumber.[22,37] From each coefficient in the derivative components, with which the observed E-A spectra can be reproduced, the electric dipole moment and molecular polarizability as well as the magnitude of the change in electric dipole moment and molecular polarizability can be determined. The above-mentioned analysis process, which may be called as the differential method, is applicable, only when the absorption bands as well as the corresponding E-A bands are fully separated to each other. If the absorption bands cannot be separated to each other or the absorption band which corresponds to the observed E-A signals cannot be identified, the differential method is inapplicable. In fact, we met with this kind of situation in the analysis of the E-A spectra of semiconductor QDs of PbSe.[38]

In the present study, PbS QDs with NIR absorption of 1100−1600 nm (corresponding to diameters of 2.5−5.0 nm) have been synthesized by a noncoordinating solvent method, and the E-A spectra of PbS QDs embedded in a poly(methyl methacrylate) (PMMA) film have been measured and analyzed. The E-A spectra of the PbS QDs in the whole spectral region could not be reproduced well by the differential method. Especially, the E-A spectra in the region between two exciton bands could not be reproduced well, as in the case of PbSe, indicating that analysis other than the differential method is necessary to understand the E-A spectra in the whole spectral region. Then, the integral method analysis of the E-A spectra of PbS has been applied to the E-A spectra of PbS, as in the case of the E-A spectra of PbSe QDs.[38]

In the integral method, the E-A spectra are integrated along the wavenumber, and the resulting spectra are fitted with the derivatives and integrals of the absorption spectra. This method is powerful to analyze the E-A spectra of PbS, especially when very weak absorption bands which show an efficient electric field effect are buried under the strong absorption background. In the present study, two absorption bands which are extremely weak in intensity and show the E-A spectra having the first derivative shape of the absorption spectrum are confirmed to be located just above the intense first exciton band. On the basis of the integral method analysis of the E-A spectra, the peak position of the newly confirmed bands as well as the magnitude of the change in polarizability following the absorption into each band is obtained as a function of the size of PbS QDs.

Differential Method Analysis and Integral Method Analysis. When an electric field ($\mathbf{F}$) is applied to molecules, each energy level is shifted by $-\mu\mathbf{F} - \alpha\mathbf{F}^2/2$, depending on μ and α of the state concerned. As a result, optical transition energy is shifted by ΔE $(= -\Delta\mu\mathbf{F} - \Delta\alpha\mathbf{F}^2/2)$, where $\Delta\mu$ and $\Delta\alpha$ are the differences in electric dipole moment and molecular polarizability, respectively, between the ground state (g) and excited state (e), i.e., $\Delta\mu = \mu_e - \mu_g$ and $\Delta\alpha = \alpha_e - \alpha_g$.[22] This is known as the Stark shift. According to the theory of electric field effects on optical spectra, the field-induced change in absorption intensity of an isotropic sample at wavenumber ν, i.e., $\Delta A(\nu)$, can be given by a sum of the zeroth, first, and second derivatives of the absorption intensity $A(\nu)$ as follows[22,23,37]

$$\Delta A(\nu) = (fF)^2\left[A_\chi A(\nu) + B_\chi \nu \frac{d}{d\nu}\left(\frac{A(\nu)}{\nu}\right) + C_\chi \nu \frac{d^2}{d\nu^2}\left(\frac{A(\nu)}{\nu}\right)\right] \quad (1)$$

Here, $F = |\mathbf{F}|$, and f is the internal field factor. E-A spectra depend on the angle between the direction of $\mathbf{F}$ and the polarization direction of electric vector of the absorption light, i.e., χ. In an immobilized and randomly distributed system, the coefficient A_χ depends on the field-induced change in transition moment. With the magic angle χ, 54.7°, B_χ and C_χ are given by the following

$$B_\chi = \frac{\Delta\bar{\alpha}}{2hc} \quad (2)$$

$$C_\chi = \frac{|\Delta\mu|^2}{6h^2c^2} \quad (3)$$

$\Delta\bar{\alpha}$ denotes the trace of $\Delta\alpha$, i.e., $\Delta\bar{\alpha} = (1/3)\mathrm{Tr}(\Delta\alpha)$. Then, it is expected that the E-A spectrum of the PbS QD is given by a linear combination of the absorption spectrum, its first and second derivatives of the absorption spectrum for each band. If the magnitude of $\Delta\mu$ following the optical absorption is significant, the presence of $\mathbf{F}$ will broaden an isolated transition, giving rise to the E-A spectrum, the shape of which is the second derivative of the absorption spectrum. If the magnitude of $\Delta\alpha$ is significant, the shape of the E-A spectrum is the first derivative of the absorption spectrum. If the transition moment is affected by $\mathbf{F}$, the E-A spectrum is similar in shape to the absorption spectrum. From eqs 2 and 3, the values of $\Delta\bar{\alpha}$ and $|\Delta\mu|$ can be obtained from the first and second derivative components of the E-A spectra, respectively.

If the E-A spectra are given by a linear combination of the zeroth, first and second derivatives of the absorption spectra, i.e., by eq 1, the integral of the E-A spectra along the wavenumber is approximately given as follows

$$\int \Delta A(\nu)\mathrm{d}\nu \cong (fF)^2\left[A_\chi \int A(\nu)\mathrm{d}\nu + B_\chi A(\nu) + C_\chi \frac{dA(\nu)}{d\nu}\right] \quad (4)$$

In the right-hand side, the first term shows a monotonic increase or decrease, as a function of wavenumber, depending on the sign of A_χ; the second term shows the spectral shape given by the absorption spectrum; and the third term shows the spectral shape given by the first derivative of the absorption spectrum. It is noted that the second and third terms must give the zero value at the tail of the integral; the nonzero value at the tail of the integral of $\Delta A(\nu)$ results from the first term of eq 4, that is, from the zeroth derivative component of the E-A spectra. Further integral of the first integral, that is, the second integral of the E-A spectra along the wavenumber, is given as follows

$$\int\{\int \Delta A(\nu)\mathrm{d}\nu\}\mathrm{d}\nu \cong (fF)^2[A_\chi \int\{\int A(\nu)\mathrm{d}\nu\}\mathrm{d}\nu + B_\chi \int A(\nu)\mathrm{d}\nu + C_\chi A(\nu)] \quad (5)$$

The first and second terms in the right-hand side show a monotonic increase or decrease, depending on the sign of A_χ

DOI: 10.1021/jp5116977
J. Phys. Chem. C 2015, 119, 4351−4361

and B_χ, while the third term shows a spectral shape which is the same as the absorption spectrum.

In the differential method, the absorption spectra must be known at the beginning. Then, the E-A spectra are simulated by the zeroth, first, and second derivatives of the absorption band. In the integral method, on the other hand, the first integral and second integral of the E-A spectra are taken. Then, the first integral should be simulated by a linear combination of the zeroth and first derivatives and the first integral of the absorption bands, and the second integral of the E-A spectrum should be simulated by a linear combination of the zeroth derivative and the first and second integrals of the absorption bands. The coefficients A_χ and B_χ can take both positive and negative values, whereas the coefficient C_χ takes only the positive value (see eq 3), indicating that spectral broadening, not spectral narrowing, is always induced by electric fields. By using the integral method, therefore, each of the E-A spectrum and its first and second integrals can be checked by comparing the simulated spectrum with the experimental data. For example, the absorption band which gives the large contribution of the second derivative component in the E-A spectrum is deduced from the second integral of the E-A spectrum. If the Stark shift is so large, the absorption band may be confirmed, even when the absorption intensity is negligibly small. Thus, the advantage of the integral method analysis is that the E-A spectra can be confirmed even when the absorption intensity is too weak to be detected, in contrast with the differential method analysis. Another advantage of the integral method is that the simulation of the E-A spectra can be done more precisely because not only the observed E-A spectrum but also its first and second integrals must be reproduced by the simulated spectra.

EXPERIMENTAL METHODS

The synthesis of PbS QDs with different sizes was performed in a three-neck flask equipped with condenser, magnetic stirrer, thermocouple, and heating mantle. A mixture of PbO, oleic acid, and octadecene (ODE), a noncoordinating solvent, was heated under Ar at 150 °C for 1 h to get the oleate precursor. A solution of bis(trimethylsilyl)sulfide (TMS) in ODE was injected into the vigorously stirring lead oleate solution at 120 °C. After the injection of TMS, the temperature of the reaction mixture was allowed to cool to 90 °C immediately for the growth of the PbS QDs. The QDs' growth process was maintained at 90 °C for 5 min. Different diameters of PbS QDs were obtained by varying the reaction time.

A certain amount of chloroform solution of a mixture of PbS QDs and PMMA was cast on an indium−tin oxide (ITO) coated quartz substrate by a spin coating method. Then, a semitransparent aluminum (Al) film was deposited on the dried polymer film by a vacuum vapor deposition technique. The ITO and Al films were used as electrodes. The X-ray diffraction (XRD) measurements were carried out on a Rigaku-Dmax 2500 diffractometer using Cu Kα radiation (λ = 0.15405 nm). The sizes of the samples were inspected using a scanning transmission electron microscope (Hitachi HD-2000 STEM). A modulation in absorption intensity was induced by a sinusoidal ac voltage with a modulation frequency of 1 kHz. A field-induced change in absorption intensity was detected with a lock-in amplifier at the second harmonic of the modulation frequency, and the dc component of the transmitted light intensity was simultaneously observed. The applied field strength was evaluated from the applied voltage divided by the thickness. E-A spectra were obtained with the same procedure as the one given in our previous papers.[39,40] The angle between the direction of the applied electric field and the electric vector of the excitation light, i.e., χ, was set to be 54.7° (magic angle) in the E-A measurements. All the measurements were done at room temperature.

RESULTS AND DISCUSSION

Absorption and E-A spectra of PbS QDs having diameters from 2.5 to 5.0 nm embedded in a PMMA film are shown in Figure 1. In order to make quantitative comparison among different

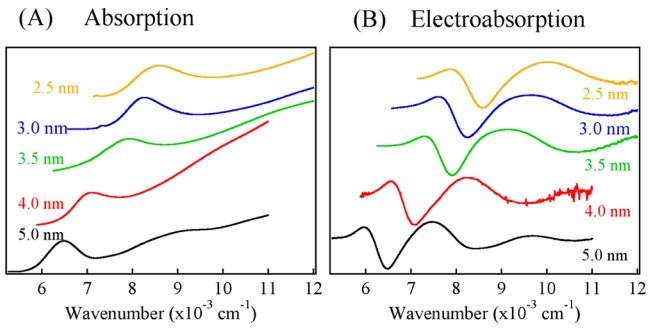

Figure 1. Absorption (A) and E-A (B) spectra for a series of PbS QDs having different sizes.

spectra, the observed E-A spectra were normalized to the one which should be obtained for the applied field strength of 0.5 MV cm^{-1}. Note that the E-A signal was confirmed to be proportional to the square of the applied electric field, in agreement with eq 1. As in the case of other semiconductor QD systems, absorption spectra of PbS QDs exhibit a blue shift, as the diameter decreases (see Figure 1). The absorption spectra demonstrate tuning of a well-resolved lowest-energy exciton transition in PbS from ~6.5 × 10^3 cm^{-1} (1538 nm) to ~8.6 × 10^3 cm^{-1} (1162 nm), which corresponds to the diameters of 5.0−2.5 nm. The generic exciton energy levels of PbS QDs has been reported by Wise and Kang.[41,42] It is suggested that the cubic rock-salt PbS QDs exhibit direct band transitions at the L point of the Brillouin zone, which is 4-fold degenerate. The energy levels of electron and hole are shown in Figure 2. The transitions usually obey the selection rule $\Delta j = 0, \pm 1$ and $\pi_e \cdot \pi_h = -1$, where j and π designate the total angular momentum and parity of the electronic state. According to these rules, the lowest absorption band corresponds to the $j = 1/2, \pi = 1 \rightarrow j = 1/2, \pi = -1$ allowed transition, and the third-lowest absorption

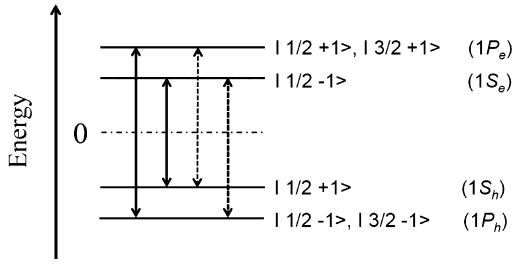

Figure 2. Generic exciton energy levels of PbS QDs, in which the states are labeled by the quantum numbers j (total angular momentum) and π (parity): $|j\pi\rangle$. The commonly used nomenclature of the levels is also shown. Allowed transitions are shown by solid arrows, while parity-forbidden transitions are shown by dotted arrows.

DOI: 10.1021/jp5116977
J. Phys. Chem. C 2015, 119, 4351−4361

band may correspond to the $j = 1/2$ or $3/2$, $\pi = -1 \rightarrow j = 1/2$ or $3/2$, $\pi = 1$ allowed transition. According to the commonly used nomenclature for the quantum confined state, the former is assigned to the $1S_h-1S_e$ transition (1S-exciton), and the latter is assigned to the $1P_h-1P_e$ transition. Note that S and P correspond to $l = 0$ and 1, respectively, where l is the orbital angular momentum, and the subscripts h and e refer to hole and electron wave functions.[43] The parity-forbidden transition $j = 1/2$, $\pi = 1 \rightarrow j = 1/2$, $3/2$, $\pi = 1$ or $j = 1/2$, $3/2$, $\pi = -1 \rightarrow j = 1/2$, $\pi = -1$, i.e., the $1S_h-1P_e$ or $1P_h-1S_e$ transition, may be partially allowed owing to asymmetry contributions and mixing of the degenerate states, and these transitions may be responsible for the second lowest absorption band(s), though the absorption intensity is expected to be very weak.[41,42] In fact, two strong exciton bands are clearly observed in the absorption region from 6000 to 13 000 cm^{-1}. These bands are denoted by G1 and G2, respectively, as described later. The peak position of these two bands with different sizes of PbS QDs is shown in Table 1.

Analysis by the Differential Method. At first, we analyzed the E-A spectra of PbS QDs with the differential method. As an example of the analysis by the differential method, the results of PbS QDs with a diameter of 5.0 nm are described. As shown in Figure 3, the absorption spectrum of PbS with a diameter of 5.0 nm observed in the region from 5000 to 11 000 cm^{-1} is regarded as a superposition of two exciton bands (G1 and G2) and the broad background whose intensity increases monotonically with increasing excitation energy. As shown in Table 1, the peak positions of G1 and G2 are at ~6500 and 8800 cm^{-1}, respectively. Then, the absorption spectrum can be decomposed into these three bands, i.e., G1, G2, and the broad background, where the absorption spectra of G1 and G2 are assumed to have a Gaussian profile; the absorption spectra are reproduced by these three bands (see Figure 3). Absorption spectra of PbS QDs having different diameters are similarly reproduced by the superposition of the bands which correspond to the first exciton band (G1), the second exciton band (G2), and the broad background, respectively. Then, we tried to simulate the E-A spectra as a sum of the zeroth, first, and second derivatives of each absorption band. Note that the first and second derivative components of each band of G1 and G2 of PbS QDs with a diameter of 5.0 nm are shown in Figure 3(B). The E-A spectrum around the G1 band is very similar in shape to the second derivative spectrum of G1, and the minimum position of the E-A spectrum around the G2 band is very close to the minimum position of the second derivative spectrum of G2, suggesting that the field-induced change in absorption spectrum primarily comes from $|\Delta\mu|$ following the transition to these two exciton states. Since the PbS QDs are embedded in rigid PMMA polymer films, the orientational effects are assumed to be negligible. The E-A signal intensity in the high wavenumber region is so weak in the observed E-A spectra, suggesting that the contribution of the broad background to the E-A spectrum is not essential. Then, the E-A spectrum was tried to be fitted by the derivative spectra of G1 and G2. In the analysis, each band of the absorption spectrum was treated independently, and the final Stark signal was taken as a sum of the E-A spectrum of each band. The second derivative component is the main contribution in the E-A spectra both for G1 and for G2. Actually, the zeroth and first derivative components were considered in the simulation of the E-A spectrum of G2. Apparently, the E-A spectrum is reproduced by a linear

Table 1. Peak Positions of G1, G2, X1, and X2 and Coefficients of A_χ, B_χ, and C_χ of Equation 1 Derived from the E-A Spectra of Different Sizes of PbS QDs with the Integral Method Analysis[a]

	G1 band		X1 band		X2 band		G2 band			
size (nm)	peak (10^3 cm^{-1})	C_χ (10^3 MV^{-2} cm^{-2})	peak (10^3 cm^{-1})	B_χ (10^3 MV^{-2} cm^{-1})	peak (10^3 cm^{-1})	B_χ (10^3 MV^{-2} cm^{-1})	peak (10^3 cm^{-1})	A_χ (10^{-2} MV^{-2})	B_χ (10^2 MV^{-2} cm^{-1})	C_χ (10^3 MV^{-2} cm^{-2})
2.5	8.62 (±0.18)	7.6 (±1.6)	9.4 (±0.5)	−1.4 (±0.5)	11.1 (±0.6)	1.2 (±0.4)	12.65 (±0.25)	5.6 (±0.5)	0 (±0.8)	8.0 (±2.6)
3.0	8.23 (±0.16)	22.9 (±4.2)	9.1 (±0.5)	−2.3 (±0.4)	10.5 (±0.5)	1.2 (±0.6)	11.38 (±0.23)	−32 (±3)	1.2 (±1.6)	9.0 (±3.0)
3.5	7.89 (±0.15)	23.5 (±5.9)	8.5 (±0.4)	−2.5 (±0.5)	10.1 (±0.5)	2.3 (±0.4)	10.75 (±0.22)	18 (±2)	0 (±0.8)	9.0 (±3.0)
4.0	7.05 (±0.14)	34.8 (±10.4)	7.8 (±0.4)	−2.9 (±0.6)	9.0 (±0.5)	2.9 (±0.6)	9.91 (±0.20)	8.8 (±0.9)	−0.6 (±1.0)	15 (±6)
5.0	6.49 (±0.13)	43.8 (±10.5)	7.2 (±0.4)	−4.4 (±0.8)	8.0 (±0.4)	4.2 (±0.8)	8.80 (±0.20)	0 (±0.1)	−8.2 (±1.6)	91 (±31)

[a]The internal field factor f is assumed to be unity, and the errors are shown in parentheses.

DOI: 10.1021/jp5116977
J. Phys. Chem. C 2015, 119, 4351−4361

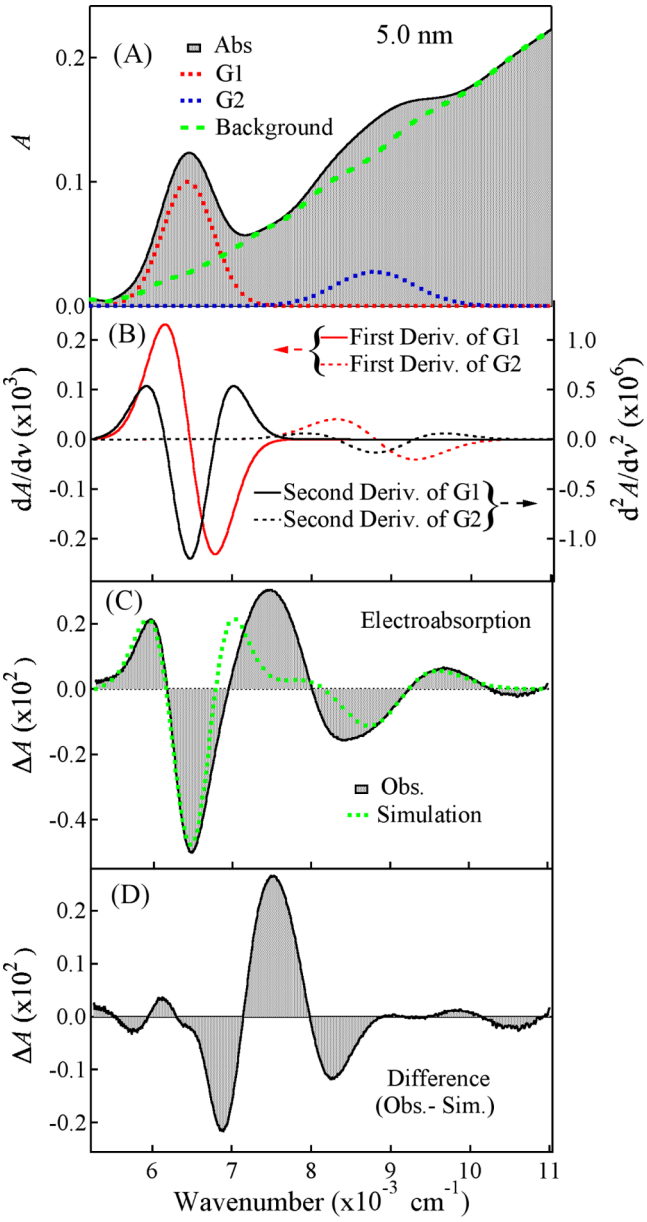

Figure 3. Differential method analysis of the E-A spectra of PbS QDs with a diameter of 5.0 nm in a PMMA film. (A) Absorption spectrum (shaded line) of PbS QDs and its decomposition to the bands G1 and G2 having the Gaussian profile and the remaining, which were used for simulation. (B) The first derivative (red line) and second derivative (black line) spectra of G1 and G2. (C) E-A spectrum (shade line) at a field strength of 0.5 MV cm^{-1} and the simulated spectrum (dotted line) derived using the differential method. (D) The difference between the observed E-A spectrum and simulated E-A spectrum shown in (C).

combination of the derivative components of the absorption bands of G1 and G2 (see Figure 3(C)). However, a careful look shows that the fitting is unsatisfactory in the region of 6500–9000 cm^{-1}, which is the region between G1 and G2. As far as only the bands G1 and G2 were considered, better fittings could not be obtained. The meaningful change was not obtained either, even when the contribution of the broad background was considered. This is true not only in PbS QDs with a diameter of 5.0 nm but also in all the PbS QDs examined in the present study. In all the cases, the satisfied fitting could not be obtained in the region between G1 and G2. The E-A spectra obtained in our Laboratory were reported by others, together with the differential method analysis.[44] As mentioned above, however, there is no doubt that other analyses are necessary to reproduce the observed E-A spectra satisfactorily.

Analysis by the Integral Method. As the origin of the disagreement between the E-A spectrum simulated by the differential method and the observed E-A spectrum, two possibilities can be pointed out: (1) absorption bands which are not observed at zero field newly appear in the presence of electric fields and (2) very weak absorption bands which are not identified in the absorption spectrum at zero field show a large electric field effect on the absorption spectrum; that is, the large Stark shift is observed for the extremely weak absorption bands.

The oscillator strength and selection rules for optical transition might be modified in the presence of electric field. For the lowest-energy transitions, for example, the 1S exciton mentioned in the foregoing part, the spatial separation of the electron and hole results in a decrease of the electron–hole overlap, and hence the oscillator strength may be affected by application of an electric field. The electric field can couple states having orbital angular momentum l and $l \pm 1$ so that transitions between states with S and P symmetry may be weakly allowed in the presence of electric fields.[45,46] In order to make clear the unsatisfactory matching between the observed and simulated spectra in the 6500–9000 cm^{-1} region of PbS QDs having a diameter of 5.0 nm, the difference between the E-A spectrum simulated by the differential method and the observed E-A spectrum was obtained, as shown in Figure 3(D). The difference does not remind the absorption band raised by the application of electric fields. Then, it is unlikely that the absorption of the unknown band is induced by the electric fields.

When the weak absorption band which is not clear in the absorption spectrum gives the large Stark shift, the integral method is powerful to analyze the E-A spectra, as shown in PbSe.[38] Then, the first integral and the second integral of the observed E-A spectrum have been taken. The results of PbS QDs with a diameter of 5.0 nm are shown in Figure 4. As mentioned already, the second integral of the E-A spectrum which corresponds to the second derivative of the absorption spectrum should show the spectrum whose shape is similar to the absorption spectrum. When the second integral of the E-A spectrum is watched from this point view, two peaks corresponding to G1 and G2 are clearly seen in Figure 4(D), in agreement with the results that the E-A spectra of G1 and G2 are similar in shape to the second derivative of the absorption spectrum. The absence of peaks other than G1 and G2 in the second integral of the E-A spectrum indicates that the absorption bands whose E-A spectra show the second derivative of the absorption spectrum are not necessary to be considered in the observed E-A spectrum, except for G1 and G2. The fact that the baseline of the second integral in the spectral region around G2 is far from zero suggests that the first derivative and/or zeroth derivative of the weak unknown absorption band contributes to the observed E-A spectrum.

The analysis by the differential method as well as the second integral of the E-A spectrum shows that the first integral of the E-A spectrum of the bands G1 and G2 must include a large contribution of the first derivative of the G1 and G2 absorption bands since the second derivative component of the absorption spectrum is dominant in the observed E-A spectrum of G1 and G2. The peak position of the lowest energy band in the second

DOI: 10.1021/jp5116977
J. Phys. Chem. C 2015, 119, 4351–4361

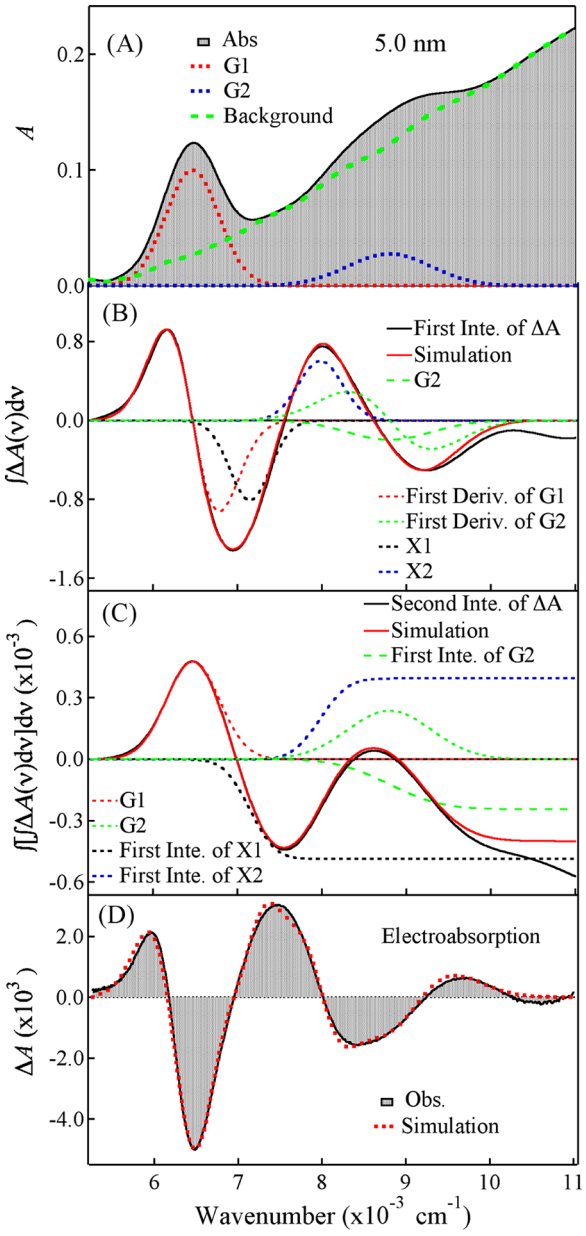

Figure 4. Integral method analysis of the E-A spectra of PbS QDs with a diameter of 5.0 nm in a PMMA film. (A) Absorption spectrum (shaded line) and G1 and G2 bands having the Gaussian profile and the remaining. (B) The first integral of the E-A spectrum (thick black solid line), simulated spectrum (thick red solid line), and the following spectra contributed to the simulated spectrum: the first derivative of G1 (red dotted line), G2 band (green broken line), the first derivative of G2 (green dotted line), X1 band (thick black dotted line), and X2 band (thick blue dotted line). (C) The second integral of the E-A spectrum (thick black solid line), simulated spectrum (thick red solid line), and the following spectra contributed to the simulated spectrum: G1 band (red dotted line), the first integral of G2 (green broken line), G2 band (green dotted line), the first integral of X1 (thick black dotted line), and the first integral of X2 bands (thick blue dotted line). (D) E-A spectrum (shaded line) at a field strength of 0.5 MV cm^{-1} and the simulated spectrum (dotted line) derived by the integral method analysis.

integral of the E-A spectrum is essentially the same as the absorption peak of G1, indicating that only the second derivative component is essential in the E-A spectrum of the G1 band. For G1, therefore, only C_χ is considered to be nonzero, and A_χ and B_χ are regarded as zero. The peak of the higher energy band in the second integral of the E-A spectrum at ~8600 cm^{-1} is significantly different from the absorption peak of G2 (~8800 cm^{-1}), indicating that not only the second derivative component of the absorption spectrum but also the zeroth- and/or first derivative components are included in the E-A spectrum of G2. If the A_χ is significant for G2, a remarkable difference should be observed between both tails of the second integral around G2 since the integral of the absorption spectrum gives a monotonic decrease or increase as a function of wavenumber, as shown in our previous paper.[38] Then, the coefficient A_χ was assumed to be zero for G2 at 5.0 nm since the second integral spectrum around G2 gives nearly the same value at both tails, while C_χ and B_χ are regarded as nonzero. The coefficient C_χ for G1 and the coefficients B_χ and C_χ for G2 have been determined by combining the differential method analysis and the integral method analysis. The results are shown in Table 1. Then, the magnitude of $\Delta\mu$ as well as $\Delta\bar{\alpha}$ was determined for G1 and G2 from the coefficients C_χ and B_χ, respectively. The results are shown in Table 2. We have to confess that the coefficients of the derivative components initially determined for the E-A spectrum of G1 and G2 are modified a little in the final stage of the simulation to reproduce well all of the E-A spectrum and its first and second integral spectra. The modified coefficients are shown in Table 1.

As shown in eqs 4 and 5, the first integral of the E-A spectrum is given by a linear combination of the zeroth and first derivatives and the first integral of the absorption bands, while the second integral of the E-A spectrum is given by a linear combination of the zeroth derivative and the first and second integrals of the absorption bands. The first integral and second integral spectra simulated for the E-A spectra with the coefficients B_χ and C_χ evaluated for G1 and G2 are shown in Figure 5, together with the integral spectrum of the observed E-A spectrum. The differences between the integral spectrum and the simulated spectrum are also shown in Figure 5, which clearly shows the presence of absorption band(s) other than G1 and G2. The difference spectrum obtained for the first integral spectra gives two bands having a positive peak at ~7970 cm^{-1} and negative peak at ~7150 cm^{-1}, respectively (see Figure 5(A)). On the other hand, the difference spectrum obtained for the second integral spectra shows one band with a negative peak at ~7570 cm^{-1}, as shown in Figure 5(B). Note that the integration is done from the low wavenumber side and that the difference spectrum is obtained by subtracting the simulated spectrum from the integral spectrum of the observed E-A spectrum.

It is possible to consider that only one weak band, whose shape is the same as the one shown in the difference spectrum of the second integral, is located between G1 and G2 (see Figure 5(B)). In that case, the field-induced spectral narrowing must be considered for this band, to interpret the observed electric field effect. As the normal electric field effect, the second derivative of the absorption spectrum resulting from the spectral broadening is expected for the E-A spectra, as mentioned in the theoretical part. Thus, the field-induced change in spectral width expected in the present study is opposite to the normal Stark effect, if only one band is assumed in the region between G1 and G2. On the basis of the first integral of the E-A spectrum, another possibility can be pointed out: two weak absorption bands exist with a peak at ~7150 and ~7970 cm^{-1}, respectively. These bands are denoted by X1 and X2, respectively. The shape of these absorption bands was

DOI: 10.1021/jp5116977
J. Phys. Chem. C 2015, 119, 4351−4361

Table 2. Magnitudes of $\Delta\mu$ for G1 and G2, i.e., $\Delta\mu_1$ and $\Delta\mu_2$, and $\Delta\bar{\alpha}$ for G2, X1, and X2, i.e., $\Delta\alpha_2$, $\Delta\alpha_{X1}$, and $\Delta\alpha_{X2}$, for Different Sizes of PbS QDs[a]

	G1 band	X1 band	X2 band	G2 band	
size (nm)	$\Delta\mu_1$ (D)	$\Delta\alpha_{X1}$ (10^4 Å^3)	$\Delta\alpha_{X2}$ (10^4 Å^3)	$\Delta\alpha_2$ (10^4 Å^3)	$\Delta\mu_2$ (D)
2.5	13 (±1)	−5.0 (±1.7)	4.3 (±1.6)	0 (±0.3)	13 (±2)
3.0	22 (±2)	−8.2 (±1.6)	4.3 (±2.0)	0.4 (±0.6)	14 (±2)
3.5	23 (±2)	−8.9 (±1.8)	8.2 (±1.6)	0 (±0.3)	14 (±2)
4.0	28 (±3)	−10.4 (±2.0)	10.4 (±2.0)	−0.2 (±0.4)	18 (±3)
5.0	31 (±3)	−15.7 (±3.0)	14.9 (±3.0)	−2.9 (±0.6)	44 (±7)

[a]The errors are shown in parentheses.

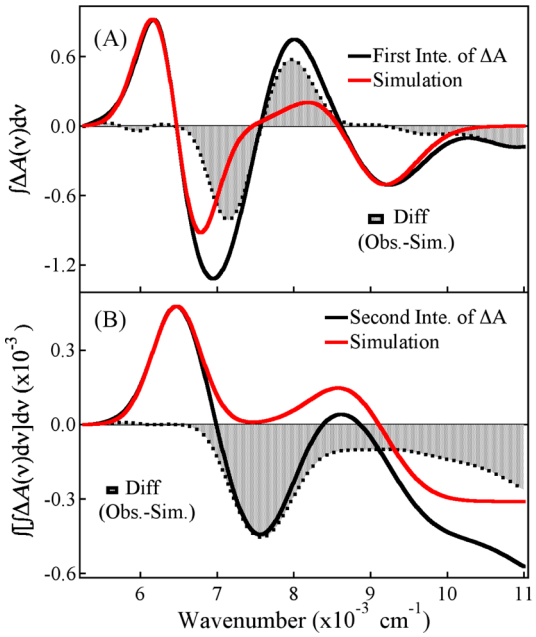

Figure 5. Integral spectra of PbS QDs with a diameter of 5.0 nm. (A) The first integral of the E-A spectrum, the simulated spectrum with G1 and G2, and the difference between the first integral spectrum and the simulated spectrum. (B) The second integral of the E-A spectrum, the simulated spectrum with G1 and G2, and the difference between the second integral spectrum and the simulated spectrum.

obtained by assuming a Gaussian profile, as shown in Figure 4(B). The E-A spectrum for each of X1 and X2 is considered to show the first derivative of the absorption spectrum in shape with the negative and positive coefficients of B_χ, respectively. These two bands become closer, as the applied field strength becomes stronger: the X1 band shows a blue-shift, whereas the X2 band shows a red-shift in the presence of **F**. Since we cannot interpret the field-induced spectral narrowing of a single absorption band at the moment, we propose that two weak absorption bands which shift closer to each other in the presence of **F** exist in the region between G1 and G2.

A large value of $\Delta\bar{\alpha}$ is obtained for both X1 and X2 bands following absorption, and only B_χ is assumed to be nonzero to simulate the E-A spectra of these two bands. The peak position of the X1 and X2 bands and the coefficients B_χ with which the E-A spectra could be fitted are shown in Table 1. Note that the coefficient B_χ was determined for X1 and X2 by assuming that the absorption intensity of these bands is one-tenth of the total absorption intensity at each peak since these bands cannot be identified in the absorption spectrum. The field-induced blue-shift of X1 and the field-induced red-shift of X2 indicate that the value of the molecular polarizability decreases following excitation at X1 and increases following excitation at X2, respectively. The magnitude of $\Delta\bar{\alpha}$, i.e., $\Delta\alpha_{X1}$ and $\Delta\alpha_{X2}$, is shown in Table 2, together with the value of $|\Delta\mu|$ for G1 and G2, i.e., $\Delta\mu_1$ and $\Delta\mu_2$. By using the coefficients of A_χ, B_χ, and C_χ for G1, G2, X1, and X2 given in Table 1, and all of the E-A spectrum and its first and second integral spectra could be reproduced quite well, as shown in Figure 4(D).

The X bands induce an extremely large change in polarizability. The dominance of the first derivative component in the E-A spectrum makes it difficult to estimate the second derivative component of the E-A spectra of these two bands, and the magnitude of $\Delta\mu$ could not be evaluated for the X1 and X2 bands.

The assignment of the second absorption peak of PbS as well as PbSe has been discussed for a long time.[43,47−50] As already reported in our previous paper, the integral method analysis of the E-A spectra of PbSe QDs shows that the extremely weak absorption band (X band in ref 38) which cannot be identified in the normal absorption spectra is buried between the first and second absorption bands, indicating that the second absorption peak is assigned to the allowed $1P_h-1P_e$ transition and that the extremely weak band X is assigned to the parity forbidden $1S_h-1P_e$ or $1P_h-1S_e$ transition. This result agrees with the one obtained on the basis of pump−probe spectroscopy and on resonant tunneling spectroscopy.[47,48] In PbS, the second peak in the optical spectra was assigned to the $1S_h-1P_e$ and $1P_h-1S_e$ transitions, based on the comparison between the scanning tunneling spectroscopy measurement and optical measurements.[50] However, the present integral method analysis of the E-A spectra of PbS QDs seems to show that the extremely weak absorption bands which cannot be identified in the absorption spectra, i.e., X1 and X2, are located between the first and second absorption bands, i.e., between G1 and G2. Therefore, the G2 band is assigned to the parity allowed $1P_h-1P_e$ transition, while X1 and X2 are assigned to the parity forbidden $1S_h-1P_e$ and $1P_h-1S_e$ transitions. The extremely large value of $\Delta\alpha_{X1}$ and $\Delta\alpha_{X2}$ may result from the transition between orbitals having different angular momentum, i.e., S and P, whose wavefuncitons give completely different distribution of electron cloud from each other. The results that only one band was confirmed between G1 and G2 in PbSe may suggest that the mixing among the above-mentioned states is not large enough to induce the splitting of the degenerated levels in PbSe, though the more anisotropic band structure, resulting in a much larger splitting of the energy levels, has been suggested in PbSe.[42]

Size Dependence of Electrical Property and Transition Energy. The integral method analysis has also been applied to the E-A spectra of PbS QDs with diameters different from 5.0 nm, and E-A spectra in the whole spectral region could be reproduced. Similar to the results of QDs having a diameter of 5.0 nm, the bands G1, G2, X1, and X2 have been

DOI: 10.1021/jp5116977
J. Phys. Chem. C 2015, 119, 4351−4361

confirmed in the absorption spectra of PbS QDs with a diameter of 2.5, 3.0, 3.5, and 4.0 nm, respectively. As shown in Figure 1, the absorption peak shifts to the red monotonically, as the size increases. The TEM images of these QDs show the narrow size dispersions (10−15%). The results of the integral method analysis of these QDs are shown in Figures S1−S4 of the Supporting Information. To simulate the E-A spectra of these samples, only the second derivative component of the absorption spectrum is taken for G1; the zeroth, first, and second derivative components are taken for G2; and only the first derivative component is taken for X1 and X2. The coefficients A_χ, B_χ, and C_χ with which the E-A spectra and its first and second integral spectra could be fitted well are shown in Table 1. Using the coefficients C_χ, the magnitude of the change in electric dipole moment for G1 and G2, i.e., $\Delta\mu_1$ and $\Delta\mu_2$, respectively, has been determined. The results are shown in Table 2. Using the coefficients B_χ, the magnitude of $\Delta\bar{\alpha}$ for the bands G2, X1, and X2, i.e., $\Delta\alpha_2$, $\Delta\alpha_{X1}$, and $\Delta\alpha_{X2}$, respectively, has been determined. The results are shown in Table 2. Again, it is noted that the absorption intensity of X1 and X2 is assumed to be one-tenth of the total intensity at the peak of these bands in any size of PbS QDs. The peak positions of the bands G1, G2, X1, and X2 are shown in Table 1 and in Figure 6(A). Plots of $\Delta\alpha_{X1}$, $\Delta\alpha_{X2}$, and $\Delta\alpha_2$ are shown in Figure 6(B) as a function of diameter of QD. Plots of $\Delta\mu_1$ and $\Delta\mu_2$ as a function of diameter of QD are shown in Figure 6(C). Note that the internal field factor, f, is assumed to be unity, i.e., $f = 1$ in eq 1. The absorption spectra of X1 and X2 obtained from the integral method analysis by assuming a Gaussian profile are also shown in Figure 7 for each size of PbS QDs, together with the observed absorption spectrum. The E-A spectra of PbS QDs in diameter of 2.5, 3.0, 3.5, and 4.0 nm could be simulated quite well by the integral method analysis in the whole spectral region (see Figures S1−S4 of the Supporting Information).

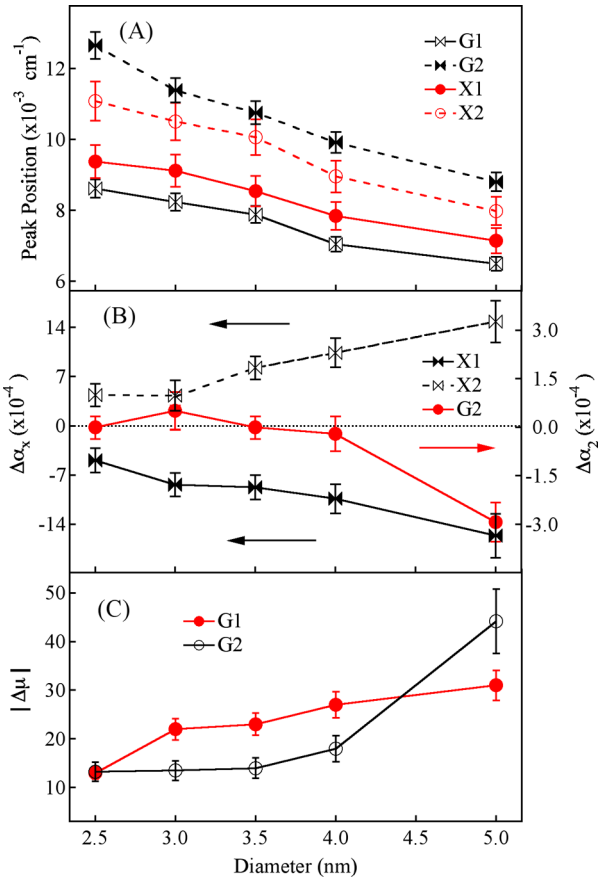

Figure 6. Plots of the physical parameters of PbS QDs as a function of diameter. (A) Peak position of the G1, G2, X1, and X2 bands, (B) the value of $\Delta\bar{\alpha}$ following absorption to the G2, X1, and X2 bands, i.e., $\Delta\bar{\alpha}_2$, $\Delta\bar{\alpha}_{X1}$, $\Delta\bar{\alpha}_{X2}$, and (C) the value of $\Delta\mu$ following absorption to the strong exciton bands G1 and G2, i.e., $|\Delta\mu_1|$ and $|\Delta\mu_2|$. The vertical line shows the error bar.

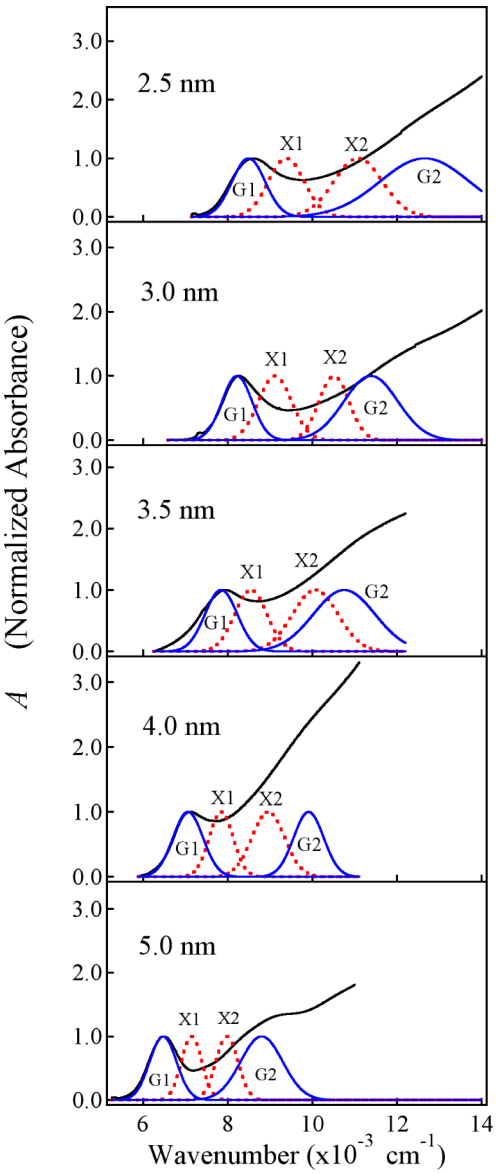

Figure 7. Spectral shape of the X1 and X2 bands newly confirmed by the integral method analysis of the E-A spectra of the PbS QDs (dotted line), along with the absorption spectra (solid line) for different diameters from 2.5 to 5.0 nm. The peak intensity of each of G1, G2, X1, and X2 is normalized in every case.

As shown in Figure 6(C), both $\Delta\mu_1$ and $\Delta\mu_2$ increase with increasing particle size; $\Delta\mu_1$ increases from 13 to 31 D, while $\Delta\mu_2$ increases from 13 to 44 D, when the diameter of PbS QDs increases from 2.5 to 5.0 nm. Since the dipole moment of any charge distribution is proportional to the distance between the electron and hole, the observed size dependence of $\Delta\mu$ suggests that the electron and hole are well separated in the excited state

DOI: 10.1021/jp5116977
J. Phys. Chem. C 2015, 119, 4351−4361

and that they move further apart as the particle size becomes larger.

The E-A spectra of PbS QDs are similar to the ones of PbSe QDs in the sense that two sharp exciton bands, which correspond to G1 and G2 of the present study, clearly show the large contribution of the second derivative component of the absorption band in the E-A spectrum. By applying the integral method analysis to the E-A spectra of PbSe QDs, it was shown that the very weak absorption band which cannot be identified in the absorption spectrum located between G1 and G2 was confirmed.[38] The finding of the unknown absorption band in the region between G1 and G2 is similar both in PbSe and in PbS. In PbSe, however, only one band which shows a blue shift in the presence of **F** was confirmed between G1 and G2.[38] In PbS, on the other hand, two bands, i.e., X1 and X2, are located between G1 and G2, though the electronic states of PbSe and PbS are considered to be very similar.

In every size of PbS QDs ranging from 2.5 to 5.0 nm in diameter, the G1 and G2 bands are assigned to the allowed transition $j = 1/2, \pi = 1 \rightarrow j = 1/2, \pi = -1$, and $j = 1/2, 3/2, \pi = -1 \rightarrow j = 1/2, 3/2, \pi = 1$, respectively. The weak bands of X1 and X2 are assigned to the parity-forbidden transition $j = 1/2, \pi = 1 \rightarrow j = 1/2, 3/2, \pi = 1$ or $j = 1/2, 3/2, \pi = -1 \rightarrow j = 1/2, \pi = -1$, whose intensity is derived by the anisotropy of the energy band, though the effect of the band anisotropy is pointed out to be quite negligible in PbS.[42] Thus, the G1 and G2 bands are assigned to the $1S_h-1S_e$ and $1P_h-1P_e$ transitions, respectively, while the X1 and X2 bands are assigned to the $1S_h-1P_e$ and $1P_h-1S_e$ transitions in every size. The mixing of the states $j = 1/2, \pi = \pm 1$ and $j = 3/2, \pi = \pm 1$ may give rise to nearly doubly degenerate levels in which one is pushed up and the other is pushed down from the original unperturbed levels, and the energies of the $1S_h-1P_e$ and $1P_h-1S_e$ transitions located below the $1P_h-1P_e$ transition may be slightly different from each other. The present results suggest that the nearly degenerated levels becomes closer to each other in the presence of **F**. The absorption intensity of the parity-forbidden transitions of $1S_h-1P_e$ and $1P_h-1S_e$ is extremely weak but not zero even at zero field. If such a breakdown of the parity selection rules as well as the splitting of the degenerated levels is caused by internal electric field in QDs,[50] the interaction between nearly degenerated levels which induces the splitting between X1 and X2 may become weaker with application of external electric fields.

The increase of the electric dipole moment in PbS QDs from 13 to 31 D for G1 and from 13 to 44 D for G2 with sizes ranging from 2.5 to 5 nm is smaller than that observed in CdSe nanocrystals, in which $|\Delta\mu|$ changes from 20 to 100 D with the CdSe nanocrystals ranging in size from 2 to 5 nm.[29] The different values of $|\Delta\mu|$ for comparable sizes of QDs may be influenced by a number of factors, such as the extent of quantum confinement (strong confinement for PbS and intermediate confinement for CdSe), crystal structure (a rock-salt crystal structure for PbS and a wurtzite crystal structure for CdSe), relative dielectric constants ($\varepsilon_r = 17$ for bulk PbS, $\varepsilon_r = 10.6$ for bulk CdSe), the density of surface states (a single dangling bond per surface atom for PbS, as many as three dangling bonds per surface atom for CdSe), and the available number of surface and defect states.[51,52] Considering the above-mentioned differences, it is not strange that the changes of dipole moments in PbS are smaller than that observed in CdSe for comparable sizes of QDs. It may be also important to note that the polar character is suggested not only in nanoparticles having wurtzite lattice but also in all nonmetal nanoparticles with surface localized charges.[52]

CONCLUSIONS

An integral method has been introduced and successfully applied to analyze the E-A spectra of PbS QDs ranging from 2.5 to 5.0 nm in diameter, which show the absorption spectra in the near-infrared region. In the results, two absorption bands (X1 and X2) which are too weak to be identified in the absorption spectrum have been newly confirmed between the two low-lying absorption bands (G1 and G2). The E-A spectra of both X1 and X2 are given by the first derivative of the absorption spectrum, and the magnitude of the change in molecular polarizability following the absorption of these bands, which increases monotonically with increasing the size of the QD at both bands, has been estimated. The peak position of all the absorption bands has been confirmed to show a red-shift with increasing size of QDs. The energy separation between the X1 and X2 bands becomes smaller in the presence of electric fields; the X1 band located in the low frequency region shows a field-induced blue-shift; while the X2 band located in the high frequency region shows a field-induced red-shift, indicating that the excited-state polarizability at the state reached by the X1 absorption is smaller than that in the ground state and that the excited-state polarizability at the state reached by the X2 absorption is larger than that in the ground state. The G1 and G2 absorption bands are assigned to the parity-allowed $1S_h-1S_e$ and $1P_h-1P_e$ transitions, respectively, while the X1 and X2 absorption bands are assigned to the parity-forbidden $1S_h-1P_e$ and $1P_h-1S_e$ transitions. Following the absorption at the G1 and G2 bands, a large change in electric dipole moment is observed, and the magnitude of the change in electric dipole moment becomes larger, as the size of PbS QDs becomes larger.

ASSOCIATED CONTENT

Supporting Information

The results of the integral method analysis of the E-A spectra of PbS QDs having a diameter of 2.5, 3.0, 3.5, and 4.0 nm, respectively, are shown in Figures S1–S4. This material is available free of charge via the Internet at http://pubs.acs.org.

AUTHOR INFORMATION

Corresponding Author

*E-mail: nohta@es.hokudai.ac.jp.

Notes

The authors declare no competing financial interest.

ACKNOWLEDGMENTS

This work was supported in part by a Grant-in-Aid for Scientific Research (Grant No. 20043005) from the MEXT in Japan.

REFERENCES

(1) Bawendi, M. G.; Steigerwald, M. L.; Brus, L. E. The Quantum Mechanics of Larger Semiconductor Clusters ("Quantum Dots"). *Annu. Rev. Phys. Chem.* **1990**, *41*, 477–496.

(2) Chan, W. C.; Nie, S. M. Quantum Dot Bioconjugates for Ultrasensitive Nonisotopic Detection. *Science* **1998**, *281*, 2016–1018.

(3) Klimov, V. I.; Mikhailovesky, A. A.; Xu, S.; Malso, A.; Hollingsworth, J. A.; Leatherdale, C. A.; Eisler, H.-J.; Bawendi, M. G. Optical Gain and Stimulated Emission in Nanocrystal Quantum Dots. *Science* **2000**, *290*, 314–317.

DOI: 10.1021/jp5116977
J. Phys. Chem. C 2015, 119, 4351–4361

(4) Coe, S.; Woo, W.-K.; Bawendi, M. G.; Bulovic, V. Electroluminescence from Single Monolayers of Nanocrystals in Molecular Devices. *Nature* **2002**, *420*, 800−803.
(5) Joo, J.; Na, H. B.; Yu, T.; Yu, J. H.; Kim, Y. W.; Wu, F.; Zhang, J. Z.; Hyon, T. Generalized and Facile Synthesis of Semiconducting Metal Sulfide Nanocrystals. *J. Am. Chem. Soc.* **2003**, *125*, 11100−11105.
(6) Achermann, M.; Petruska, M. A.; Kos, S.; Smith, D. L.; Koleske, D. D.; Klimov, V. I. Energy-Transfer Pumping of Semiconductor Nanocrystals Using an Epitaxial Quantum Well. *Nature* **2004**, *429*, 642−646.
(7) Thessing, J.; Qian, J.; Chen, H.; Pradhan, N.; Peng, X. Interparticle Influence on Size/Size Distribution Evolution of Nanocrystals. *J. Am. Chem. Soc.* **2007**, *129*, 2736−2737.
(8) Talapin, D. V.; Lee, J. S.; Kovalenko, M. V.; Shevchenko, E. V. Prospects of Nanocrystal Solids as Electronic and Optoelectronic Materials. *Chem. Rev.* **2010**, *110*, 389−458.
(9) Alivisatos, P. The Use of Nanocrystals in Biological Detection. *Nat. Biotechnol.* **2004**, *22*, 47−52.
(10) Zrazhevskiy, P.; Sena, M.; Gao, X. Designing Multifunctional Quantum Dots for Bioimaging, Detection, and Drug Delivery. *Chem. Soc. Rev.* **2010**, *39*, 4326−4354.
(11) Nozik, A. J.; Beard, M. C.; Luther, J. M.; Law, M.; Ellingson, R. J.; Johnson, J. C. Semiconductor Quantum Dots and Quantum Dot Arrays and Applications of Multiple Exciton Generation to Third-Generation Photovoltaic Solar Cells. *Chem. Rev.* **2010**, *110*, 6873−6890.
(12) Du, H.; Chen, C.; Krishnan, R.; Krauss, T. D.; Harbold, J. M.; Wise, F. W.; Thomas, M. G.; Silcox, J. Optical Properties of Colloidal PbSe Nanocrystals. *Nano Lett.* **2002**, *2*, 1321−1324.
(13) Sargent, E. H. Infrared Quantum Dots. *Adv. Mater.* **2005**, *17*, 515−522.
(14) Mao, S.; Zhao, J.; Zhang, S.; Niu, H.; Jin, B.; Tian, Y. Synthesis and Electrochemical Properties of PbSe Nanotubes. *J. Phys. Chem. C* **2009**, *113*, 18091−18096.
(15) Koole, R.; Allan, G.; Delerue, C.; Meijerink, A.; Vanmaekelbergh, D.; Houtepen, A. J. Optical Investigation of Quantum Confinement in PbSe Nanocrystals at Different Points in the Brillouin Zone. *Small* **2008**, *4*, 127−133.
(16) Lifshitz, E.; Bashouti, M.; Kloper, V.; Kigel, A.; Eisen, M. S.; Berger, S. Synthesis and Characterization of PbSe Quantum Wires, Multipods, Quantum Rods, and Cubes. *Nano Lett.* **2003**, *3*, 857−862.
(17) Quen, Z. W.; Li, C. X.; Zhang, X. M.; Yang, J.; Yang, P. P.; Zhang, C. M.; Lin, J. Polyol-Mediated Synthesis of PbS Crystals: Shape Evolution and Growth Mechanism. *Cryst. Growth Des.* **2008**, *8*, 2384−2392.
(18) Pietryga, J. M.; Werder, D. J.; Williams, D. J.; Casson, J. L.; Schaller, R. D.; Klimov, V. I.; Hollingsworth, J. A. Utilizing the Lability of Lead Selenide to Produce Heterostructured Nanocrystals with Bright, Stable Infrared Emission. *J. Am. Chem. Soc.* **2008**, *130*, 4879−4885.
(19) Hines, M. A.; Scholes, G. D. Colloidal PbS Nanocrystals with Size-Tunable Near-Infrared Emission: Observation of Post-Synthesis Self-Narrowing of the Particle Size Distribution. *Adv. Mater.* **2003**, *15*, 1844−1849.
(20) Buckingham, A. D. In *Medical Technical Publishing Company International Review of Science*; Physical Chemistry, Series 1; Ramsay, D. A., Ed.; Butterworth: London, 1972; Vol. 3, p 73.
(21) Hochstrasser, R. M. Electric Field Effects on Oriented Molecules and Molecular Crystals. *Acc. Chem. Res.* **1973**, *6*, 263−269.
(22) Liptay, W. In *Excited States*; Lim, E. C., Ed.; Academic Press: New York, 1974; Vol. *1*, pp 129−229.
(23) Bublitz, G. U.; Boxer, S. G. Stark Spectroscopy: Application in Chemistry, Biology, and Materials Science. *Annu. Rev. Phys. Chem.* **1997**, *48*, 213−242.
(24) Empedocles, S. A.; Bawendi, M. G. Quantum-Confined Stark Effect in Single CdSe Nanocrystallite Quantum Dots. *Science* **1997**, *278*, 2114−2117.
(25) Hache, F.; Ricard, D.; Flytzanis, C. Quantum-Confined Stark Effect in Very Small Semiconductor Crystallites. *Appl. Phys. Lett.* **1989**, *55*, 1504−1506.
(26) Ohara, Y.; Nakabayashi, T.; Iwasaki, K.; Torimoto, T.; Ohtani, B.; Hiratani, T.; Konishi, K.; Ohta, N. Electric-Field-Induced Changes in Absorption and Emission Spectra of CdS Nanoparticles Doped in a Polymer Film. *J. Phys. Chem. B* **2006**, *110*, 20927−20936.
(27) Merbach, D.; Schöll, E.; Ebeling, W.; Michler, P.; Gutowski, J. Electric-Field-Dependent Absorption of ZnSe-Based Quantum Wells: The Transition from Two-Dimensional to Three-Dimensional Behavior. *Phys. Rev. B* **1998**, *58*, 10709−10720.
(28) Colvin, V. L.; Alivisatos, A. P. CdSe Nanocrystals with a Dipole Moment in the First Excited State. *J. Chem. Phys.* **1992**, *97*, 730−733.
(29) Colvin, V. L.; Cunningham, K. L.; Alivisatos, A. P. Electric Field Modulation Studies of Optical Absorption in CdSe Nanocrystals: Dipolar Character of the Excited State. *J. Chem. Phys.* **1994**, *101*, 7122−7138.
(30) Sacra, A.; Norris, D. J.; Murray, C. B.; Bawendi, M. G. Stark Spectroscopy of CdSe Nanocrystallites: The Significance of Transition Linewidths. *J. Chem. Phys.* **1995**, *103*, 5236−5245.
(31) Menendez-Proupin, E.; Trallero-Giner, C. Electric-Field and Exciton Structure in CdSe Nanocrystals. *Phys. Rev. B* **2004**, *69*, 125336−1∼9.
(32) Ohshima, R.; Nakabayashi, T.; Kobayashi, Y.; Tamai, N.; Ohta, N. External Electric Field Effects on State Energy and Photoexcitation Dynamics of Water Soluble CdTe Nanoparticles. *J. Phys. Chem. C* **2011**, *115*, 15274−15281.
(33) Nakabayashi, T.; Ohshima, R.; Ohta, N. Electric Field Effects on Photoluminescence of CdSe Nanoparticles in a PMMA Film. *Crystals* **2014**, *4*, 152−167.
(34) Stokes, K. L.; Persans, P. D. Excited States and Size-Dependent Electro-Optical Properties of CdS_xSe_{1-x} Quantum Dots. *Phys. Rev. B* **1996**, *54*, 1892−1901.
(35) Klem, E. J. D.; Levina, L.; Sargent, E. H. PbS Quantum Dot Electroabsorption Modulation across the Extended Communications band 1200−1700nm. *Appl. Phys. Lett.* **2005**, *87*, 053101−1∼3.
(36) Liu, X. M.; Iimori, T.; Ohshima, R.; Nakabayashi, T.; Ohta, N. Electroabsorption Spectra of PbSe Nanocrystal Quantum Dots. *Appl. Phys. Lett.* **2011**, *98*, 161911−1∼3.
(37) Jalviste, E.; Ohta, N. Theoretical Foundation of Electroabsorption Spectroscopy: Self-Contained Derivation of the Basic Equations with the Direction Cosine Method and the Euler Angle Method. *J. Photochem. Photobiol. C: Photochem. Rev.* **2007**, *8*, 30−46.
(38) Awasthi, K.; Iimori, T.; Ohta, N. Integral Method Analysis of Electroabsorption Spectra and Its Application to Quantum Dots of PbSe. *J. Phys. Chem. C* **2014**, *118*, 18170−18176.
(39) Jalviste, E.; Ohta, N. Stark Spectroscopy of Indole and 3-Methylindole Embedded into a Polymethylmethacrylate Film: Field Induced Orientation Effect. *J. Chem. Phys.* **2004**, *121*, 4730−4739.
(40) Tayama, J.; Iimori, T.; Ohta, N. Comparative Study of Electroabsorption Spectra of Polar and Non-polar Organic Molecules in Solution and in a Polymer Film. *J. Chem. Phys.* **2009**, *131*, 244509−1∼7.
(41) Wise, F. W. Lead Salt Quantum Dots: the Limit of Strong Quantum Confinement. *Acc. Chem. Res.* **2000**, *33*, 773−780.
(42) Kang, I.; Wise, F. W. Electronic Structure and Optical Properties of PbS and PbSe Quantum Dots. *J. Opt. Soc. Am. B* **1997**, *14*, 1632−1646.
(43) Nootz, G.; Padilha, L. A.; Olszak, P. D.; Webster, S.; Hagan, D. J.; Van Stryland, E. W.; Levina, L.; Sukhovatkin, V.; Brzozowski, L.; Sargent, E. H. Role of Symmetry Breaking on the Optical Transitions in Lead-Salt Quantum Dots. *Nano Lett.* **2010**, *10*, 3577−3582.
(44) Liu, X.; Lü, Y.; Dai, Z.; Tang, X.; Yan, L. Electroabsorption Spectra of Lead Sulfide (PbS) Quantum Dots in a Polymer Film. *J. Phys. Chem. C* **2013**, *117*, 21483−21489.
(45) Andreev, A. D.; Lipovskii, A. A. Anisotropy-Induced Optical Transitions in PbSe and PbS Spherical Quantum Dots. *Phys. Rev. B* **1999**, *59*, 15402−15404.

DOI: 10.1021/jp5116977
J. Phys. Chem. C 2015, 119, 4351−4361

(46) Xia, J. Electronic Structures of Zero-Dimensional Quantum Wells. *Phys. Rev. B* **1989**, *40*, 8500−8507.
(47) Trinh, M. T.; Houtepen, A. J.; Schins, J. M.; Piris, J.; Siebbeles, L. D. A. Nature of the Second Optical Transition in PbSe Nanocrystals. *Nano Lett.* **2008**, *8*, 2112−2117.
(48) LiIjeroth, P.; van Emmichoven, P. A. Z.; Hickey, S. G.; Weller, H.; Grandidier, B.; Allan, G.; Vanmaekelbergh, D. Density of States Measured by Scanning-Tunneling Spectroscopy Sheds New Light on the Optical Transitions in PbSe Nanocrystals. *Phys. Rev. Lett.* **2005**, *95*, 086801−1∼4.
(49) Ellingson, R. J.; Beard, M. C.; Johnson, J. C.; Yu, P.; Micic, O. I.; Nozik, A. J.; Shabaev, A.; Efros, A. L. Highly Efficient Multiple Exciton Generation in Colloidal PbSe and PbS Quantum Dots. *Nano Lett.* **2005**, *5*, 865−871.
(50) Diaconescu, B.; Padilha, L. A.; Nagpal, P.; Swartzentruber, B. S.; Klimov, V. I. Measurement of Electronic States of PbS Nanocrystal Quantum Dots using Scanning Tunneling Spectroscopy: The Role of Parity Selection Rules in Optical Absorption. *Phys. Rev. Lett.* **2013**, *110*, 127406−1∼5.
(51) Rabani, E.; Hetenyi, B.; Berne, B. J.; Brus, L. E. Electronic Properties of CdSe Nanocrystals in the Absence and Presence of a Dielectric Medium. *J. Chem. Phys.* **1999**, *110*, 5355−5369.
(52) Shim, M.; Guyot-Sionnest, P. Permanent Dipole Moment and Charges in Colloidal Semiconductor Quantum Dots. *J. Chem. Phys.* **1999**, *111*, 6955−6964.

DOI: 10.1021/jp5116977
J. Phys. Chem. C 2015, 119, 4351−4361